Proceedings of 3ICIP:
3rd International Conference on Inverse Problems in Engineering
June 13-18, 1999, Port Ludlow, WA

3ICIP27

PARAMETER IDENTIFICATION OF RADIATIVE AND CONDUCTIVE HEAT TRANSFER IN THE SINTERING GLASS MATERIALS

Sergey V. Reznik, Dmitry Yu. Kalinin, Andrey M. Mikhalev,
Pavel V. Prosuntsov, Andrey V. Shulakovsky
Bauman Moscow State Technical University
Dept. M-1, 5, 2nd Baumanskaya street, Moscow, 107005, Russia
Phone: (7-095) 263–67–05, Fax: (7-095) 261–01–07, 261–36–14
E-mail: sreznik@serv.bmstu.ru

ABSTRACT

The problem of radiative and conductive heat transfer (RCHT) parameter identification in the sintering glass materials (SGM) produced by sintering of disperse glass particles is considered. The structure and properties of SGM considerably change during sintering: from the pouring of loose particles of more than 40 percent porosity at the initial state to the solid material of less than 3 percent porosity at the final state. The authenticity of heat transfer mathematical models in such materials is of great importance for optimization of manufacturing methods and new equipment design.

The RCHT mathematical model, which considers combined behavior of heat transfer, radiation absorption and scattering, porous material shrinkage, thermal and optical properties dependencies from temperature and porosity has been developed. An extremal statement of coefficient inverse problem (IP) was suggested for this model's parameters identification. The solution algorithm is based on the nongradient minimization method. The peculiarities of RCHT parameter identification by thermal experiment results were analyzed by means of the numerical simulation.

NOMENCLATURE

Greek letters

α – heat transfer coefficient (W m^{-2} K^{-1})
ε – emissitivity
ξ – relative radius of interparticle contact
η – shear viscosity coefficient (Pa s)
Λ – wavelength (μm)
Λ_S – semi-transparent wavelength band (μm)
Λ_O – opaque wavelength band (μm)
λ – heat conduction coefficient (W m^{-1} K^{-1})
ν – parameter in eq. (13), (14)
σ – specific surface tension (Pa)
ρ – density (kg m^{-3})
τ – time (s)
τ_f – duration of heating (s)

Latin letters

A – surface absorptivity factor
c – specific heat capacity (J kg^{-1} K^{-1})
B – Plank function (W m^{-2}·μm^{-1})
D – radiation diffusion coefficient (m)
E – spectral density of radiation (W m^{-2} μm^{-1})
k – absorption coefficient (m^{-1})
L – thickness of layer (m)
$\bar{L}$ – carcass parameter of interpenetrative structure
M – layer mass per unit mass (kg m^{-2})
N_τ – number of time steps of finite difference net
N_t – number of temperature sensors
n – refraction index
P – porosity
q_1 – spectral density of incident radiative flux (W m^{-2} μm^{-1})
q_R – spectral density of radiative flux (W m^{-2} μm^{-1})
q_V – rate of internal heat sources (W kg^{-1})
R_{ef} – effective hemispheric surface reflection coefficient
r_p – average particle radius (m)
s – spatial Lagrange mass coordinate (kg m^{-2})
T – temperature (K)
T_g – surround medium temperature (K)
x – spatial Euler coordinate (m)

Subscripts/Superscripts

0 – initial moment of time
1 (2) – front (back) surface
e – experimental value
t – temperature sensor

INTRODUCTION

The thermal sintering of glass powder is a very attractive manufacturing technology for various products, such us facing materials, filters, heat insulation [1]. The gradient structure of desired density distribution may be obtained by this technology. We have to consider the following phenomena for optimization of glass powder sintering modes during developing of the heat transfer mathematical model:

- Combined behavior of heat transfer in the glass that belongs to the semi-transparent materials in the range of $\Lambda_S = 0{,}8 - 4{,}4\ \mu\text{m}$.
- Sintering material macrostructure transformations, which influences whole set of the physical properties of SGM, in particular, thermal and optical properties. At that, the 50 percent porosity of the initial state decreases to zero porosity of the final state.
- Microstructure phenomena, such as viscous flow under surface tension, which finally cause macrostructure transformations.

The empiric methods, rough mathematical models and approximate thermal properties were recently widely used for determination of SGM heat treatment modes. The same questions were discussed in the frames of investigations of metal powder sintering [2], heat protection systems [3], thermal properties of composite materials [4–6]. However, the mathematical model considering the above phenomena had not been developed.

The developing of mathematical model is inseparable from the modeling of the required media properties. There are two approaches of heterogeneous media parameter determination. The first way is based on study of microstructure and mechanisms of heat transfer between microstructure's component of the elemental representative volume. The second way includes experimental tests of specimens and unknown parameter identification by the IP solution.

PHYSICAL MODEL

It is assumed that heat transfer takes place in the flat layer (fig. 1). The plate has following initial parameters: L_0, ρ_0, $T_0(x)$, $P_0(x)$. The layer properties are constant in the surfaces, which are parallel to the boundaries. The incident diffusive radiative flux of $q_1(\tau)$ density acts on the top boundary. There are two opaque and diffusive reflective shields on the each layer sides. The layer material is semi-transparent. The material volumetrically absorbs and scatters radiation in the semi-transparent band Λ_S. The material absorbs radiation on the surface within opaque band Λ_O. A material shrinkage takes place during heating. The $M = \rho_0 \cdot L_0$ layer mass does not change. An external forces influence and gas discharge do not take place. The thermal properties depend on the temperature and porosity. The optical properties depend on the wavelength, porosity and temperature.

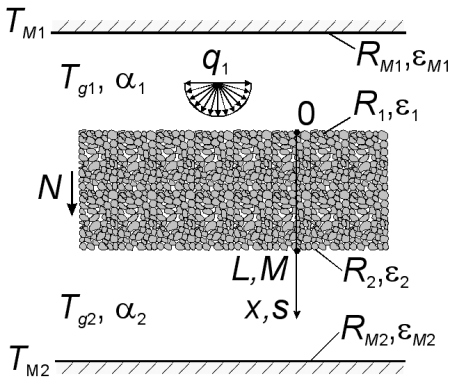

Figure 1. To the problem statement

MATHEMATICAL MODEL

The RCHT mathematical model includes energy equation and equation of radiation diffusion, initial and boundary conditions, sintering equations and additional relations.

The Lagrange coordinate connected to layer mass movement has been used for energy equation notation. In this case we do not need the continuity equation, in contrast to Euler coordinate. The transition from Euler coordinate to Lagrange coordinate is provided by mass coordinate s in following form

$$s_A = \int_0^{x_A} \rho \, \mathrm{d}x, \tag{1}$$

where s_A, x_A – Lagrange and Euler coordinate of some point A located within layer.

The governing energy equation can be expressed as

$$c\frac{\partial T}{\partial \tau} = \frac{\partial}{\partial s}\left(\lambda \rho \frac{\partial T}{\partial s}\right) + q_V, \quad 0 \le s \le M, \quad 0 \le \tau \le \tau_f; \tag{2}$$

initial condition

$$T = T_0, \quad 0 \le s \le M; \tag{3}$$

boundary conditions

$$-\lambda \rho \frac{\partial T}{\partial s} = \int_{\Lambda_O} \left(A_1 q_1(\tau) - \varepsilon_1 B\right) \mathrm{d}\Lambda + \alpha_1 \left(T_{g1} - T\right), \quad s = 0, \quad 0 \le \tau \le \tau_f; \tag{4}$$

$$\lambda \rho \frac{\partial T}{\partial s} = -\int_{\Lambda_O} \varepsilon_2 B(T) \mathrm{d}\Lambda + \alpha_2 \left(T_{g2} - T\right), \quad s = M, \quad 0 \le \tau \le \tau_f. \tag{5}$$

The rate of internal heat sources that arise from radiative flux absorption is calculated from

$$q_V = \frac{\partial q_R}{\partial s} = \int_{\Lambda_s} \frac{k\,n^2}{\rho}(E - B)\,\mathrm{d}\Lambda\,. \qquad (6)$$

Spectral density of radiation E, which is necessary for solution of eq. (6), can be obtained by the following equation of radiation diffusion

$$-\frac{\partial}{\partial s} D n^2\, \rho \frac{\partial E}{\partial s} + \frac{k\,n^2}{\rho} E = \frac{k\,n^2}{\rho} B, \quad 0 \le s \le M, \quad 0 \le \tau \le \tau_f; \qquad (7)$$

with boundary conditions

$$-D\,\rho \frac{\partial E}{\partial s} + \frac{(1 - R_{ef})}{(1 + R_{ef})} E = 2\frac{(1 - R_{ef})}{(1 + R_{ef})} q_1(\tau), \quad s = 0, \quad 0 \le \tau \le \tau_f; \qquad (8)$$

$$D\,\rho \frac{\partial E}{\partial s} + \frac{1}{2}\frac{(1 - R_{ef})}{(1 + R_{ef})} E = 0, \quad s = M, \quad 0 \le \tau \le \tau_f. \qquad (9)$$

The system (7)–(9) describes the process of radiation transfer in the semi-transparent scattering media in the form by V. Petrov [7].

The information about porosity distribution in the layer being considered is necessary for equations (2)–(9). When the external forces influence is negligible, the basic mechanism of shrinkage is viscous flow of the substance under the capillar forces. In addition, the porous material is packed by means of free surface energy decreasing. In this case, the model developed by V. Scorokhod [2] may be used

$$P(\tau, s) = P_0 \exp\left(-\frac{9}{4} \int_0^{\tau} \frac{\sigma\,\mathrm{d}\,\tau'}{r_p \cdot \eta} \right). \qquad (10)$$

The calculation of heat conduction coefficients also is in need of relative radii of interparticle contacts (fig. 2).

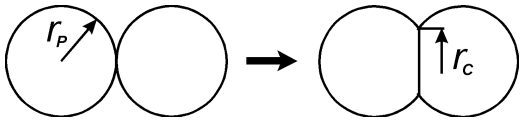

Figure 2. Scheme of the particles junction and appearance of the contact area

According to V. Scorokhod [2], if the same mechanism of viscous flow determines both local deformations of the contact area (i.e. growth of contact size) and global deformation of the whole porous body (i.e. shrinkage) the relative radius of interparticle contact area is found by

$$\xi^2 = (r_c / r_p)^2 = 1 - (P/P_0)^{4/3}. \qquad (11)$$

PHYSICAL PROPERTIES PRESENTATION

The density can be expressed as

$$\rho(T, P) = \rho_0(T)(1 - P). \qquad (12)$$

The heat conduction coefficient of SGM is a property of total heat transfer that considers temperature dependencies of heat conductivity of the different phases and structural parameters (porosity, particles size and particles asperity). The influence of these parameters is not without ambiguity. From one side, the interparticle contact area and conductive component of effective heat conductivity increase during particle softening and junction. From another side, the energy part that is transferred by filling gas decreases during sintering.

The large difference between initial and final states of structure points out that the description of heat transfer mechanisms must contain several parts corresponding to different structure states. There are a lot of works devoted to the investigations of heterogeneous material heat conductivity, for example, A. Misnar [4], G. Dulnev and Yu. Zarichnyak [5], Ye. Litovsky and N. Puchkelevich [6].

Two mathematical models of heat conductivity of sintering material describing the material state from pouring of loose particles to the nonporous sintered material have been employed in the paper presented.

The pouring of loose particles has random packing of homogeneous structure (fig.3a). However, when the porosity exceeds 40 percent the regions of big pores appear in the pouring. The junction of particles leads to the structure of the same behavior during heating. The pores in SGM become isolated at the final state and their volume decreases (fig.3b).

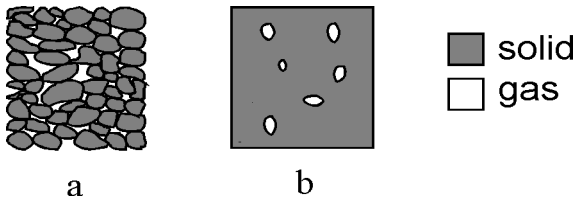

Figure 3. Schematic view of SGM structure for different states: a – pouring of loose particles; b – sintered material

The interpenetrative structure model was developed by G. Dulnev [5]. This model consists of particles' chaotic packing and spatial pores net. The model takes into account heat transfer through contact area, gap between particles and continuous pores

$$\lambda = \lambda_s \left(\bar{L}^2 + \nu(1 - \bar{L})^2 + 2\nu\bar{L}(1 - \bar{L})(\nu\bar{L} + 1 - \bar{L})^{-1} \right), \qquad (13)$$

where $\nu = \lambda_g / \lambda_s$.

When material has a small number of isolated pores the model by [5] can be used

$$\lambda = \lambda_s \left(1 - \frac{P}{(1 - \nu)^{-1} - (1 - P)/3} \right). \qquad (14)$$

The smoothing of the heat conduction coefficient, which is calculated by eq. (13), (14), is realized in the 30–40-percent porosity band.

The techniques of semi-transparent material optical properties calculation, which take into account structural parameters, have been developed by Moiseev S.S. et al [8], L. Dombrovsky [9]. These properties were considered known in the paper presented.

SOLUTION ALGORITHM OF DIRECT PROBLEM

An implicit finite difference grid have been employed for numerical solution of system (2)–(5). The usage of Lagrange mass coordinate makes for simpler numerical solution because the finite difference grid will not change during shrinkage.

The multigroup approximation has been applied for consideration of spectral dependence during solution of equation of radiation diffusion.

For determination of temperature and porosity distributions the following procedure have been used on the each time step:

1. Calculation of spatial distribution of porosity and relative interparticle radius by integrating eq. (10) and substituting of porosity values into eq. (11).
2. Calculation of density distribution by eq. (12).
3. Determination of the rate of internal heat sources by solution eq. (7)–(9) and (6).
4. Calculation of the Euler coordinates of the spatial grid nodes by means of inverting eq. (1).
5. Calculation of heat conduction coefficients at the spatial grid nodes under eq. (13) and (14).
6. Determination of temperature field by the eq. (2)–(5).
7. Test of convergence conditions for temperature and porosity.
8. Repetition from step 1 in case of non-satisfied convergence conditions.
9. Consideration of next time step.

INVERSE PROBLEM STATEMENT

The accuracy of mathematical modeling of RCHT in SGM greatly depends on the authenticity of the physical properties being used. The standard experimental equipment, which is based on contact heating of specimens, is good for the states of investigated materials when the structural transformations are absent. On the contrary, the changes of specimen form and size, the contact fault between cell's measuring elements lead to the great instrumental and methodical errors. In addition, the measurements with standard equipment are carried out under the steady state or regular heat transfer with low rates. This fact hinders the study of influence of real kinetics of the thermal properties changes.

The inverse methods of thermal properties identification under conditions of convective or radiative heating have been developed by J. Beck [10], O. Alifanov et al [11]. These methods lift restrictions on the mobility of the specimen boundaries. The methods [12, 13] that allow identifying thermal properties of semi-transparent scattering materials within wide temperature band have also been developed by authors of the paper presented. These methods provide a division of conductive and radiative transfer contributions in the specimens with immovable boundaries. In this connection, the developing of new experimental techniques and data processing methods, which join unique abilities of methods above, is very urgent.

Among all properties of SGM, the heat conduction coefficient has a greatest influence on the temperature gradient and, therefore, on the structure gradient forming. One of the possible experiment schemes for measurement of heat conduction coefficient is presented on fig. 4. The temperature sensors are fixed in measuring cell body and do not move during sintering and material shrinkage (fig. 5). During experimental data processing, we have to use the information of temperature sensors (fig. 6) with consideration of differences in the time of sensor being in the layer, heating rates and temperature level.

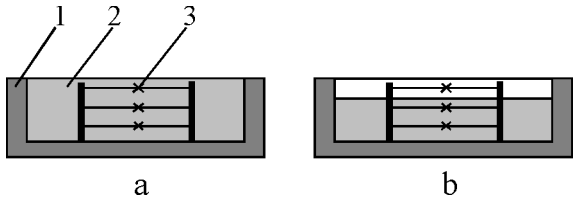

Figure 4. Temperature sensors arrangement scheme for heat conduction coefficient measurement: a – before sintering; b – during sintering; 1 – measuring cell body; 2 – glass powder; 3 – thermocouple

IP is formulated in extremal statement in conformity with experiment conditions described above: to determine $\lambda(T)$, which leads to minimum of residual between calculated and experimental temperatures

$$J(\vec{u}) = \sum_{i=1}^{N_t} \int_0^{\tau^e} w_i(\tau)\left(T^c(x_{t,i},\tau) - T_i^e(\tau)\right)^2 \mathrm{d}\tau, \qquad (15)$$

$$\vec{u} = \left\{\lambda(T),\ \forall T \in \left[T_0^e,\ T_{\max}^e\right]\right\},$$

where x_i – co-ordinate of i-th sensor; $w_i(\tau) = \begin{cases} 1 & \tau \le \tau_i^t \\ 0 & \tau > \tau_i^t \end{cases}$ – weight function; τ_i^t – duration of i-th sensor being within the layer.

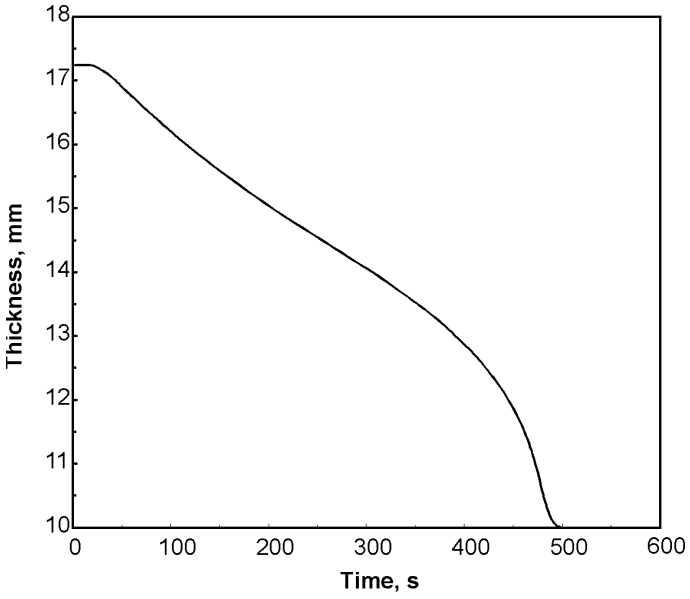

Figure 5. Change of sintering layer thickness

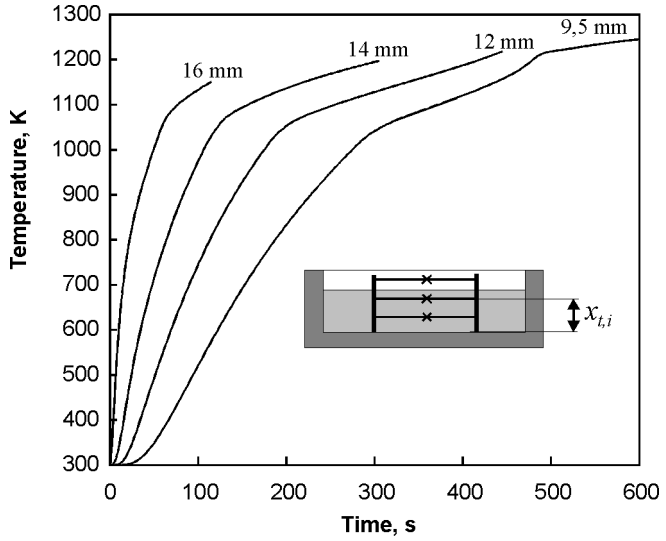

Figure 6. Temperature histories of sensors being located at the different distance from bottom boundary

The desired dependence $\lambda(T)$ is presented as

$$\lambda(T) = \sum_{k=1}^{K} p_k \varphi_k; \qquad (16)$$

where p_k – identified parameters; φ_k – basis functions; K – given number of parameters.

The linear splines are used as basis functions for eq. (16). The quantity of basis functions is chosen adjusted with temperature dependence of shear viscosity. We may pick out three typical domain in the $\eta(T)$: domain of solid state bounded by flow temperature, where $\eta>10^7$ Pa·s; transient domain where $10^7>\eta>10^4$ Pa·s and low viscosity domain where $\eta<10^4$ Pa·s. The junction process runs with high velocity in the last domain, and we can consider nonporous material. Thus, the quantity of temperature domain (i.e. basis functions) can not be less then three, i.e. $K \geq 3$.

The following function is minimized instead of functional (15) during IP solution

$$J = \sum_{i=1}^{N_t} \sum_{j=1}^{N_\tau} w_i(\tau_j)\left(T_i^e(\tau_j) - T^c(x_i,\tau_j)\right)^2 \Delta\tau_j . \qquad (17).$$

The gradient methods have proved good for IP solutions. However, the calculation of target function gradient takes the time-consumimg operation of adjoint problem building that can write in analytical or difference form for each new mathematical model. For function (15) minimization, the nongradient method of deformed-polyhedron by D. Himmelblau [14] is used in the paper presented .

The restrictions on minimal and maximal values of $\lambda(T)$ is given as

$$\lambda_{\min} \leq \lambda(T) \leq \lambda_{\max}, \quad T \in \left[T^e_{\min}, T^e_{\max}\right], \qquad (18)$$

where $\lambda_{\min}, \lambda_{\max}$ – given a priori values.

In case of exact data usage for $\lambda(T)$ identification, the minimization process terminates when polyhedron is reduced to a given size (in the order of 10^{-5}). In case, the experimental data content errors the minimization process terminates under following condition

$$J \leq \sum_{i=1}^{N_t} \sum_{j=1}^{N_\tau} w_i(\tau_j)\delta^2 \Delta\tau_j , \qquad (19)$$

where δ – error of temperature measurement.

NUMERICAL EXPERIMENTS

The inverse algorithm efficiency has been tested by some numerical experiments. The heat conductivity of hypothetical disperse material has been identified. The material properties of disperse particles were close to the properties of natrium–lime–silica glass. The layer made of these particles was 17,25-mm initial thickness. The initial porosity was constant and equal to 42 percent. The layer had been heated by constant radiative flux of $1{,}5\cdot10^5$ W/m^2 density. The spectral distribution of the flux was given as Plank black body function of 1300 K temperature. The division by four domains within the semi-transparent band $\Lambda_S = [0{,}8; 4{,}4]$ μm has been used for optical properties description.

The estimation of unknown function has been carried out by temperature history of one sensor being at the 9,5-mm distance from bottom in the first run of the numerical experiment. The sensor was located within layer boundaries at all times. The quantity of temperature domain varied from 4 to 8. The firs run results are presented in fig. 7(a). The exact

dependence $\lambda(T)$ presented on the fig.7(a) and 7(b) was calculated by eq. (13) and (14).

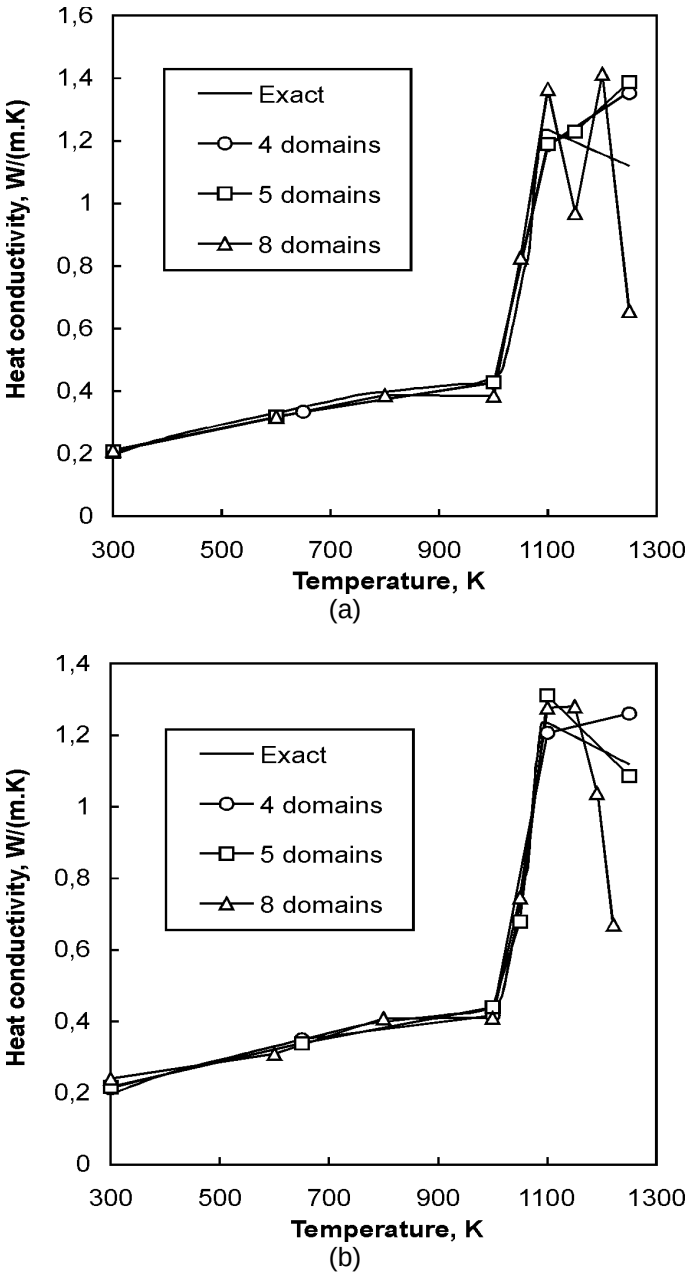

Figure 7. Estimated $\lambda(T)$ by the information of one (a) and two (b) temperature sensor for different number of temperature domains

As could be seen, there is a good coincidence between given and estimated $\lambda(T)$ within low temperature domain, i.e. before sintering. The estimation error does not exceed 2–3 percent. The results within high temperature domain are satisfactory too; however, the oscillations of estimated dependence take place when the quantity of temperature domains is growing.

Apparently, we may explain it by the insufficiency of information about high temperature domain, because the sensor is located too far from heated boundary during the time of the experiment.

We have used temperature histories of two sensors for $\lambda(T)$ estimation in the second run. One of them was the same. Another one has been located closer to the heated boundary at the 14-mm distance from bottom. However, the temperature history of the second sensor has been considered only to 300-th second, i.e. until it was located within sintering layer. The results of the second run, presented on fig. 7(b), demonstrate better results and oscillation absence within high temperature domain.

The influence of random errors on the $\lambda(T)$ estimation has been studied in the third run. The random errors distributed under the normal low of 1-percent standard deviation have been added to initial temperatures. The estimation of heat conduction coefficient was carried by two sensors. The obtained results (fig. 8) demonstrate good stability of developed algorithm.

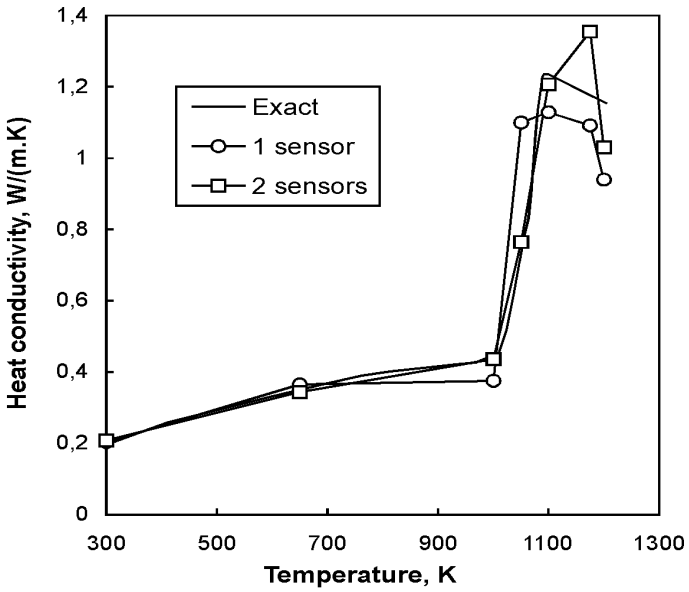

Figure 8. Estimated $\lambda(T)$ in case of 1-percent random errors

CONCLUSION

1. The mathematical model of RCHT in the sintering semi-transparent scattering material was presented.

2. For parameter identification of RCHT model, an extremal statement of coefficient IP was suggested. The algorithm of IP solution is based on the nongradient method of target function minimization.

3. The algorithm stability to the random errors and sensors quantity has been studied by the numerical experiments.

ACKNOWLEDGMENTS

This research was supported by INTAS (Grant YSF98-130) and Ministry of Education of Russian Federation.

REFERENCES

1. Sarkisov, P.D. Directional crystallization – Basis of Versatile Glass-crystal Material Production. Mendeleev Russian University on Chemical Technology, Moscow, 1997. (In Russian)

2. Skorokhod, V.V. Rheological Basics of Sintering Theory. Naukova dumka, Kiev, 1972. (In Russian)

3. Polezhaev, Yu.V., Yurevich F.B. Heat Protection.– Energiya, Moscow, 1976. (In Russian)

4. Missenard, A. Conductivite Thermique des Solides, Liuides, Gaz et de Leurs Melanges. Editions Eyrolles, Paris, 1965. (In French)

5. Dulnev, G.N., Zarichnyak, Yu.P. Heat Conductivity of Mixtures and Composite Materials. Energiya, Moscow, 1974. (In Russian)

6. Litovsky, Ye. Ya., Puchkelevich, N.A. Thermal Properties of Heat-resistant Materials. Handbook. Metallurgiya, Moscow, 1982. (In Russian)

7. Petrov, V.A. Complex Approach to a Radiative-conductive Heat Transfer Problem in Scattering Semi-transparent Material Using a Diffusive Approximation as the Base. *J. of Engineering Physics and Thermophysics*, 1993, no. 6.

8. Moiseev, S.S., Petrov, V.A., Stepanov S.V. Optical Properties of High-temperature Fibrous Silica Thermal Insulation. *High Temperatures – High Pressures*, vol. 24, 1992, 391–402.

9. Dombrovsky, L.A. Radiation Heat Transfer in Disperse Systems. Begell House Inc. Publ., New York, 1996.

10. Beck, J.K., Blackwell, B., Clair, C.R.Jr. Inverse Heat Conduction Ill-posed Problems. A Wiley-Interscience Publication, New York, 1985.

11. Alifanov, O.M., Artyukhin, E.A., Rumyantsev, S.V. Extreme Methods of Solving Ill-posed Problems. Begeel House, New York, 1995.

12. Prosuntsov, P.V., Reznik, S.V. Determination of the Thermophisical Properties of Translucent Material. *J. of Engineering Physic*, 1985, vol.49, no.6, 1458–1462.

13. Reznik, S.V. Inverse Problems and Parameters Determination of Heat Transfer in Semi-transparent Media. *Final report of Joint American-Russian NSF Workshop on Inverse Problems in Heat Transfer*, Beck J.V., Alifanov O.M. co-principal organizers, East Lansing (Mi), 1992, P.B.10.1–B.10.16.

14. Himmelblau, D.M. Applied Nonlinear Programming. McGraw-Hill, New York, 1972.